AD-A129 483 PROPERTIES OF ACTUAL AND NUMERICAL SHOCK AND BLAST WAVE 1/1
PHENOMENA(U) TORONTO UNIV DOWNSVIEW (ONTARIO) INST FOR
AEROSPACE STUDIES I I GLASS APR 83 ARO-16972.11-EG
UNCLASSIFIED DAAG29-80-C-0077 F/G 19/4 NL

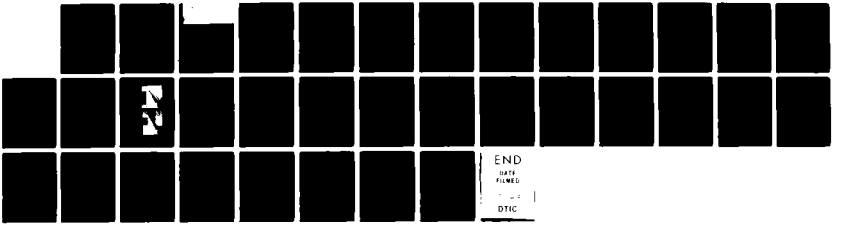

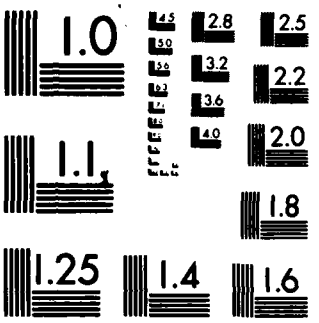

MICROCOPY RESOLUTION TEST CHART
NATIONAL BUREAU OF STANDARDS-1963-A

Unclassified

SECURITY CLASSIFICATION OF THIS PAGE (When Data Entered)

REPORT DOCUMENTATION PAGE

READ INSTRUCTIONS BEFORE COMPLETING FORM

1. REPORT NUMBER: 16972.11-EG	2. GOVT ACCESSION NO.
3. RECIPIENT'S CATALOG NUMBER	
4. TITLE (and Subtitle): Properties of Actual and Numerical Shock and Blast Wave Phenomena	5. TYPE OF REPORT & PERIOD COVERED: Final: 1 Mar 80 - 28 Feb 83
6. PERFORMING ORG. REPORT NUMBER	
7. AUTHOR(s): I. I. Glass	8. CONTRACT OR GRANT NUMBER(s): DAAG29 80 C 0077
9. PERFORMING ORGANIZATION NAME AND ADDRESS: University of Toronto, Downsview, Ontario, Canada M3H 5T6	10. PROGRAM ELEMENT, PROJECT, TASK AREA & WORK UNIT NUMBERS
11. CONTROLLING OFFICE NAME AND ADDRESS: U. S. Army Research Office, Post Office Box 12211, Research Triangle Park, NC 27709	12. REPORT DATE: Apr 83 13. NUMBER OF PAGES: 31
14. MONITORING AGENCY NAME & ADDRESS (if different from Controlling Office)	15. SECURITY CLASS. (of this report): Unclassified 15a. DECLASSIFICATION/DOWNGRADING SCHEDULE

16. DISTRIBUTION STATEMENT (of this Report)

Approved for public release; distribution unlimited.

17. DISTRIBUTION STATEMENT (of the abstract entered in Block 20, if different from Report)

18. SUPPLEMENTARY NOTES

The view, opinions, and/or findings contained in this report are those of the author(s) and should not be construed as an official Department of the Army position, policy, or decision, unless so designated by other documentation

19. KEY WORDS (Continue on reverse side if necessary and identify by block number)

random choice
explosions
implosions
shock waves
blast waves
detonations
shock tube studies

20. ABSTRACT (Continue on reverse side if necessary and identify by block number)

Considerable progress was made in the areas of application of the random-choice method to explosion and implosion dynamics (flows with changes in area and detonation) and weak spherical shock-wave transitions (flows with viscosity, heat conduction, and vibrational excitation - a first). Some progress was also made in applying the fluid-in-cell technique to oblique-shock-wave reflections (OSWR). The method looks promising. A great deal of experimental and analytical work was achieved on OSWR in air and SF_6. The dusty-gas shock tube is being assembled. Two analytical papers on dusty-gas shock-tube flows have appeared in the Proceedings of the Royal Society of London with AFOSR support, as well as other papers and UTIAS reports.

DD FORM 1 JAN 73 1473 EDITION OF 1 NOV 65 IS OBSOLETE

UNCLASSIFIED

SECURITY CLASSIFICATION OF THIS PAGE (When Data Entered)

INSTITUTE
FOR
AEROSPACE STUDIES

UNIVERSITY OF TORONTO

FINAL REPORT ON

"PROPERTIES OF ACTUAL AND NUMERICAL SHOCK AND BLAST WAVE PHENOMENA"

Research Agreement No. DAAG29-80-C-0077

March 1, 1980 - February 28, 1983

by

Dr. I. I. Glass
Principal Investigator

DISCLAIMER NOTICE

THIS DOCUMENT IS BEST QUALITY PRACTICABLE. THE COPY FURNISHED TO DTIC CONTAINED A SIGNIFICANT NUMBER OF PAGES WHICH DO NOT REPRODUCE LEGIBLY.

UNIVERSITY OF TORONTO
INSTITUTE FOR AEROSPACE STUDIES
4925 DUFFERIN ST.
DOWNSVIEW, ONTARIO, CANADA, M3H 5T6
TEL. 667-7700

FINAL REPORT ON "PROPERTIES OF ACTUAL AND NUMERICAL SHOCK AND BLAST WAVE PHENOMENA"

Research Agreement No. DAAG29-80-C-0077

1 MAR., 1980 - 28 FEB., 1983

by

Dr. I. I. Glass, Principal Investigator

1) Abstract

Considerable progress was made in the areas of application of the random-choice method to explosion and implosion dynamics (flows with changes in area and detonation) and weak spherical shock-wave transitions (flows with viscosity, heat conduction, and vibrational excitation - a first). Some progress was also made in applying the fluid-in-cell technique to oblique-shock-wave reflections (OSWR). The method looks promising. A great deal of experimental and analytical work was achieved on OSWR in air and SF_6. The dusty-gas shock tube is being assembled at a slow pace owing to a lack of funds (support from ARO was terminated in February and some funds promised by AFWL have also not been forthcoming. Consequently, Canadian money that could have gone into dusty-gas shock-tube equipment is now being used for salaries and operating expenses of a reduced research and technical staff). Two analytical papers on dusty-gas shock-tube flows have appeared in the Proceedings of the Royal Society of London with AFOSR support, as well as other papers and UTIAS reports.

2) Objectives

Our objectives were to provide analytical, numerical and experimental dat

OSWR in pure and dusty gases. The results can prove to be invaluable in verifying complex two and three-dimensional codes used for nuclear explosions and height-of-burst chemical-explosive experiments. Our isopycnic, pressure and interferometric data can establish an important base for testing these complex codes so that they can become credible before many millions of dollars are spent in running routine and unproven numerical results.

3. Description of Accomplishments

and

4. Publications

No better elaboration can be given of the Abstract on the accomplishments achieved during the past 36 months than through the various publications. A summary and a figure of each is enclosed:

a) "On a Dusty-Gas Shock Tube" by Miura and Glass, Proc. R. Soc. Lond., A382, 373-388, 1982.

b) "On the Passage of a Shock Wave Through a Dusty-Gas Layer" by Miura and Glass, Proc. R. Soc. Lond., A385, 85-105, 1983.

c) "Temperature Measurements at an Implosion Focus" by Saito and Glass, Proc. R. Soc. Lond., A384, 217-231, 1982.

d) "An Update on Non-Stationary Oblique Shock-Wave Reflections: Actual Isopycnics and Numerical Experiments" by Deschambault and Glass, J. Fluid Mech., to be published 1983.

e) "An Assessment of Recent Results on Pseudo-Stationary Oblique-Shock-Wave Reflections", by Shirouzu and Glass, UTIAS Report No. 264, 1982.

f) "Domains and Boundaries of Pseudo-Stationary Oblique Shock-Wave Reflections", by J.-H. Lee and I. I. Glass, UTIAS Report No. 202, 1982.

g) "Random-Choice Solutions for Spherical Shock-Wave Transitions

of N-Waves in Air with Vibrational Excitation" by H. Honma and I. I. Glass, UTIAS Report No. 253, 1982.

h) "An Experimental, Analytical and Numerical Study of Temperatures Near Hemispherical Implosion Foci", by T. Saito, UTIAS Report No. 260, 1982 - Also U. of T. Thesis (Ph.D.).

i) "Numerical Analysis of Dusty Supersonic Flow Past Remote Axisymmetric Bodies", by H. Sugayama, UTIAS Report No. 267, 1983.

5. Professional Personnel

Prof. I. I. Glass - Principal Investigator

Dr. J. J. Gottlieb - Coinvestigator

Prof. H. Honma - Visiting Professor (Japan)

Dr. J.-H. Lee - Postdoctoral Fellow (Japan)

Dr. H. Miura - Postdoctoral Fellow (Japan)

Mr. M. Shirouzu - Senior Research Engineer (Japan)

Dr. T. Saito - Ph.D. Candidate and Postdoctoral Fellow (Japan)

M.A.Sc. Candidates

John Hu (Hong Kong)

John Wheeler (Canada)

Fred Wong (Hong Kong)

Technicians (Part Time)

Mr. A. Morte

Mr. D. Wilmut

6. DOD Scientific Interactions

a) Dr. Wes Kitchens and Mr. John Keefer, BRL, can verify the significance of our work on shock-wave reflection in pure and dusty gases - especially air, in providing an analytical, numerical and experimental data base.

b) The same can be said of Dr. George Ullrich, DNA, Dr. J. Wilson,

AFOSR, and Dr. Harland Glaz, NSWC.

c) In the industrial sector: Dr. Allen Kuhl of R & D Associates, Dr. Harold Brode of Pacific Sierra Research, Dr. Charles Needham, S-Cubed and Dr. John Kurylo, Physics International.

d) Additional confirmation can be obtained from Dr. Phillip Colella, Lawrence Berkeley Laboratory and Dr. Paul Kutler, NASA Ames.

7. Specific Technical Applications

Without our work unchecked field-trial explosion-data and numerical analyses would be accepted as correct at face value. Now, field-test data and numerical results can be constructively scrutinized by comparison to our work and the correctness of the physical meaning of all data can be properly assessed.

Proc. R. Soc. Lond. A 382, 373-388 (1982)
Printed in Great Britain

On a dusty-gas shock tube

BY H. MIURA† AND I. I. GLASS

Institute for Aerospace Studies, University of Toronto,
4925 Dufferin Street, Downsview, Ontario, Canada M3H 5T6

(*Communicated by A. D. Young, F.R.S. – Received* 10 *December* 1981)

Analytical and numerical methods were used to investigate the flow induced by a shock wave in a shock-tube channel containing air laden with suspended small solid particles. Exact results are given for the frozen and equilibrium shock-wave properties as a function of diaphragm-pressure ratio and shock-wave Mach numbers. The driver contained air at high pressure. A modified random-choice method together with an operator-splitting technique show clearly both the decay of a discontinuous frozen shock wave and a contact discontinuity, and the formation of a stationary shock structure and an effective contact front of finite thickness.

The effects of particle diameter, particle-number density and diaphragm-pressure ratio on the transitional behaviour of the flow are investigated in detail. The alteration of the flow properties owing to the presence of particles is discussed thoroughly and compared with classical shock-tube flows.

1. INTRODUCTION

When a gas carries many solid particles, they significantly affect the flow through the transfer of momentum and heat from or to the gas. Shock waves propagating in such a dusty gas are characterized by a transition region orders thicker than that caused by viscosity and heat conduction in a pure gas. Across the transition front, the interaction of the gas and the particles leads to an equilibrium state of the mixture. The structure of stationary shock waves has been studied theoretically on the assumption that the formulae for the drag and the rate of heat transfer for a single spherical particle placed in a steady flow can still be applied to the motion of many particles contained in a dusty gas (Carrier 1958, Marble 1963, Kriebel 1964, Rudinger 1964, Miura 1972).

Shock waves were studied experimentally in a dusty gas inside a shock tube to obtain some data on the interaction of the two phases (Crowe *et al.* 1963, Selberg & Nicholls 1968, Rudinger 1970, Outa *et al.* 1976). Some of the results showed an effective drag coefficient, obtained from the observation of the acceleration of the particles behind the shock waves, that differed appreciably from that for a single particle. However, there were many factors influencing the results and a definitive conclusion on the appropriate drag coefficient to be used is not available as yet.

Recently, numerical analyses followed these experimental studies. The shock-

† Permanent address: College of Engineering, University of Osaka Prefecture, Sakai, Japan.

...he shock front, however, are still fairly large at this stage. These must ...with time (Miura 1972) and the extent of the shock transition will elongate. ..., the shock relaxation length or time is larger for larger mass concentration. ...inally, the effect of the presence of particles upon the stationary shock waves is discussed based on the idealized equilibrium-flow limit. The pressure p_2 of the gas in the uniform region behind the shock-transition region satisfies the classical shock-tube equation (Glass & Hall 1959)

$$\frac{p_4}{p_1} = \frac{p_2}{p_1}\left[1 - \frac{(\gamma_4 - 1)(a_1/a_4)(p_2/p_1 - 1)}{(2\gamma_1)^{\frac{1}{2}}\{2\gamma_1 + (\gamma_1 + 1)(p_2/p_1 - 1)\}^{\frac{1}{2}}}\right]^{-2\gamma_4/(\gamma_4 - 1)}, \tag{25}$$

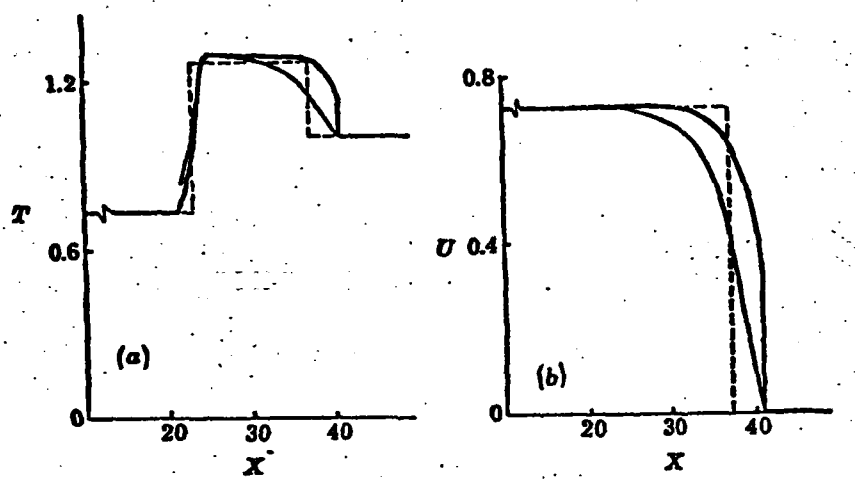

FIGURE 5. Flow quantities at $\tau = 32$ ($\alpha = 1$, $P_{41} = 10$, $d = 40$ μm): (*a*) temperature; (*b*) velocity. Thick lines, gas; thin lines, particles; dashed lines, equilibrium flow.

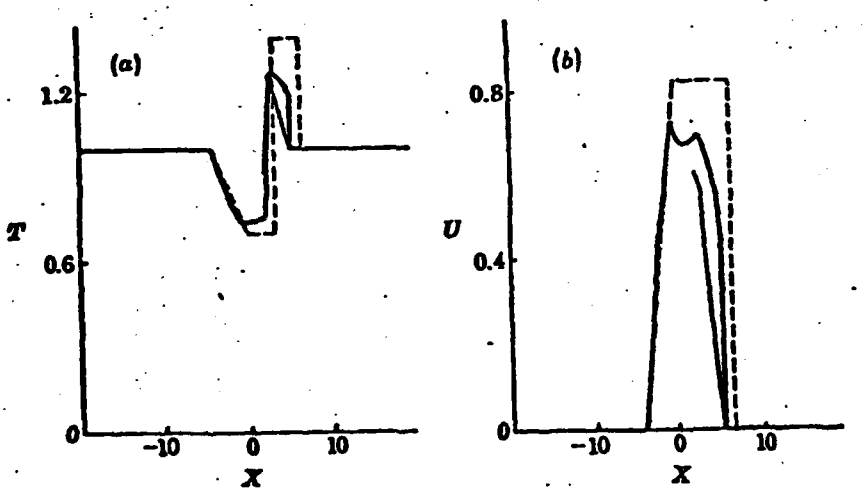

FIGURE 6. Flow quantities at $\tau = 4$ ($\alpha = 2$, $P_{41} = 10$, $d = 10$ μm): (*a*) temperature; (*b*) velocity. Thick lines, gas; thin lines, particles; dashed lines, frozen flow.

Proc. R. Soc. Lond. A 385, 85–105 (1983)
Printed in Great Britain

On the passage of a shock wave through a dusty-gas layer

BY H. MIURA† AND I. I. GLASS‡

† *College of Engineering, University of Osaka Prefecture, Sakai, Japan*
‡ *Institute for Aerospace Studies, University of Toronto, Toronto, Canada*

(*Communicated by A. D. Young, F.R.S. – Received 20 May 1982*)

[Plate 1]

The flow resulting from the passage of a shock wave through a dusty-gas layer is studied theoretically. On the basis of an idealized equilibrium-gas approximation, the criteria for the wave reflexion at the contact surface separating the pure gas from the dusty-gas layer are obtained in terms of the properties of the gas and the dusty gas. For the cases treated here, a shock wave is reflected at the first contact surface and a shock wave stronger than the incident one is transmitted into the dusty-air layer. Subsequently, a rarefaction wave is reflected at the second contact surface and the shock wave transmitted into the free air is weakened by this non-linear interaction. The induced rarefaction wave reflects later at the first contact surface as a compression wave, which runs through the layer to overtake the transmitted shock wave in air. The final emergent shock wave from the dusty air has almost the same strength as the original shock wave entering the layer.

The time-dependent transition properties through the shock waves, contact surfaces and rarefaction waves are found by solving the equations of motion numerically by a modified random-choice method with an operator-splitting technique.

1. INTRODUCTION

High speed flows of a mixture of a gas and small solid particles are encountered in several branches of engineering and science (see, for example, Marble 1970, Boothroyd 1971; Rudinger 1980). Shock waves in such a dusty gas exhibit relaxation features typical of two-phase flow. For sufficiently strong shock waves, a discontinuous jump in the gas phase precedes a thick transition region. A non-equilibrium state of the mixture gives way gradually to an equilibrium transition through the transfer of momentum and heat between the gas and the particles. This feature was used in experimental studies, with a shock tube, for an understanding of the basic mechanisms of the interaction between the two phases (Crowe *et al.* 1963, Selberg & Nicholls 1968, Rudinger 1970). For example, effective drag coefficients of the particles were deduced from the experimental results, but their values cannot as yet be considered definitive.

Some experiments used a shock tube in which only a limited portion of the channel away from a diaphragm was filled with a dusty gas (Outa *et al.* 1976, Lowenstein &

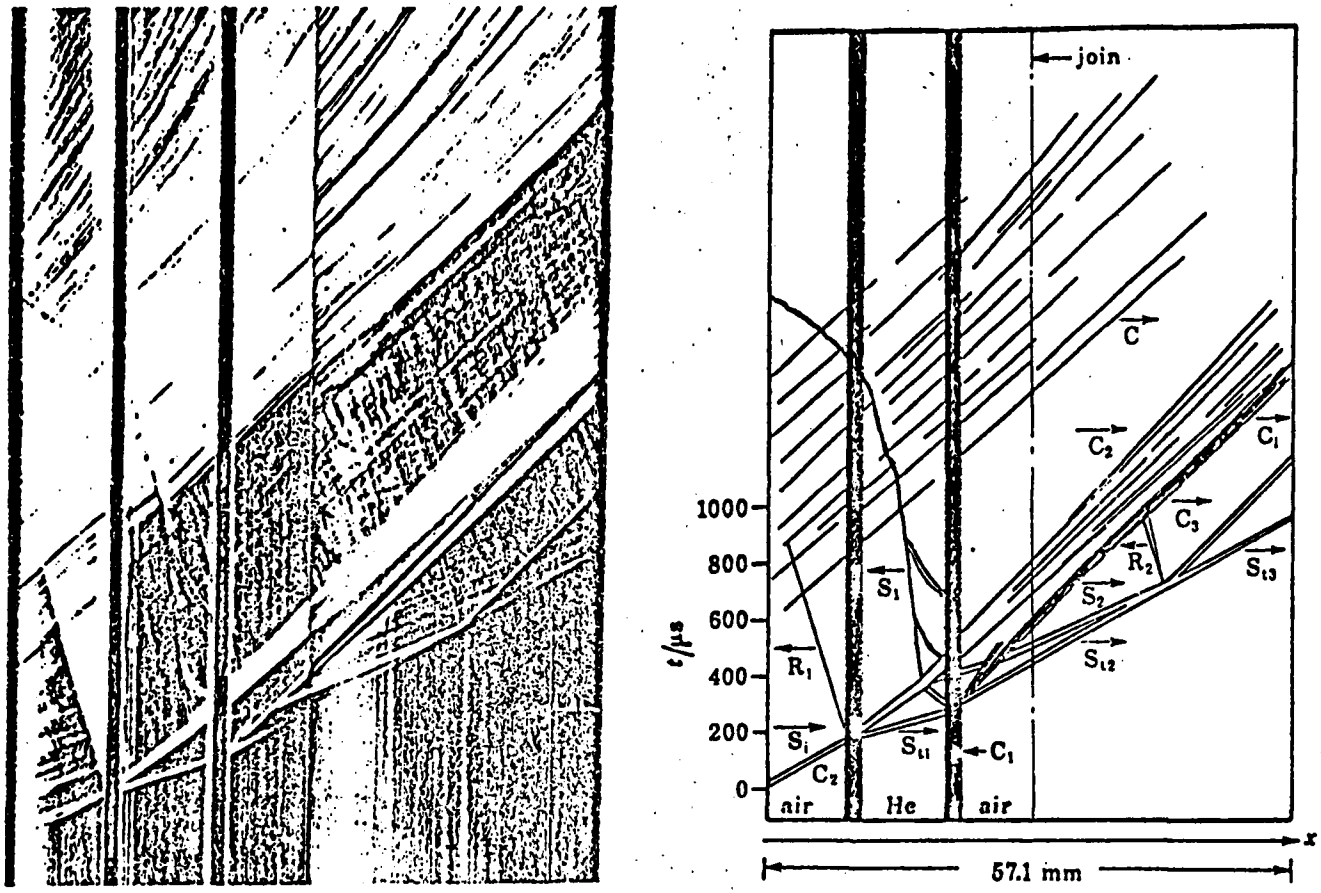

FIGURE 1. Schlieren record of distance–time (x, t) plane and explanatory sketch of the passage of an air shock wave through a layer of helium in a 7.6 × 7.6 cm² wave-interaction tube. The undisturbed gases are initially at room temperature (293 K) and atmospheric pressure. The incident shock wave S_i, in air, refracts into helium at the microfilm contact surface C_2, causing a transmitted shock wave S_{11}, and a reflected rarefaction wave R_1. The transmitted shock wave S_{11} refracts into air at the microfilm contact surface C_1, generating a transmitted shock wave S_{12}, and a reflected shock wave S_1, which refracts at C_2, producing a reflected shock wave S_2, which overtakes S_{12}. This gives rise to the final shock wave S_{13}, a perfect contact surface C_2 (unlike C, produced by the bursting diaphragm), and a very weak reflected rarefaction wave R_2. The initial refraction at C_2 causes shock S_i to attenuate in pressure ratio in the helium layer. The second refraction at C_1 amplifies the pressure ratio of S_{12} in air. However, owing to the nonlinearity of the refractions, S_{12} is weaker than S_i. The overtaking of S_2 and S_{12} amplifies S_{13} so that it is nearly the same strength as S_i. Note the rapid diffusion of the helium–air contact surfaces at C_1 and C_2. Mach numbers of S_i = 1.70, S_{12} = 1.66 and S_{13} = 1.69; pressure ratio across R_2 = 0.97.

(Facing p. 86)

Proc. R. Soc. Lond. A 384, 217–231 (1982)
Printed in Great Britain

Temperature measurements at an implosion focus

BY T. SAITO AND I. I. GLASS

Institute for Aerospace Studies, University of Toronto, 4925 Dufferin Street, Downsview, Ontario, Canada M3H 5T6

(*Communicated by A. G. Gaydon, F.R.S. – Received* 28 *May* 1982)

Spectroscopic temperature measurements were made at the focal point of imploding shock waves in the UTIAS implosion chamber, which has a 20 cm diameter hemispherical cavity. The chamber was filled with a stoichiometric H_2–O_2 gas mixture at different initial pressures (1.4–6.9 MPa). The mixture was ignited at the origin by an exploding wire generating an outgoing detonation wave, which reflected at the chamber wall as an imploding shock wave (gas runs). Experiments with an explosive shell of pentaerythritol tetranitrate (PETN: $C_5H_8N_4O_{12}$) placed at the hemispherical wall were also conducted. The shell was detonated by the impact of the reflected gaseous detonation wave at its surface, an intense implosion wave being generated thereby (explosive run). The temperatures were measured at the implosion focus by using a medium quartz Hilger spectrograph with an eight-photocell polychromator attachment over the visible wavelength range. The measured radiation intensity distributions were fitted to black-body curves. The temperatures were 10000–13000 K, for gas runs, and 15000–17000 K, for explosive runs. The continuous spectra from photographic film and the measured emissivities, which were very close to unity, confirmed that the plasma was a black body. Numerical studies with the random choice method and classical strong-shock theory were used to analyse the flows in the entire range of the implosion process. They provided much information on the entire implosion process within the restriction of a perfect-gas assumption, which was found to be reasonable as a first step in this kind of analysis. The experimental data were compared with the analytical results. For both gas and explosive runs, the temperatures were lower than the calculated values and reasonable explanations are given for this deviation.

INTRODUCTION

The UTIAS explosive-driven implosion chamber has been used in several research areas since it was conceived by Glass (1972) in the early 1960s. The extremely high pressures and temperatures generated at the focus of implosions were used for driving projectiles to hypervelocities (Flagg & Glass 1968), as a shock-tube driver (Glass *et al.* 1974), and to produce diamonds (Glass & Sharma 1976). Most recently, experimental studies were done on deuterium–deuterium fusion reactions and on measurements of the neutrons and γ-rays generated by the reaction (Glass & Sagie 1982).

The conditions produced by imploding spherical shock waves were first obtained by Guderley (1942). His self-similar solutions, however, deal only with very strong

in γ is very difficult to take into account and in the present study it was assumed that γ was constant ($\gamma = 1.14$) in the region of interest (*ca.* 0.55 mm). Real-gas effects at this point were shown to have a negligible effect.

Comparison of experimental results and analysis

Figure 12 compares the experimental results and the expected average temperatures over a 0.55 mm diameter circular area at the origin. The calculated temperature depends on the position of the imploding shock wave. When the wave radius is larger than the radius of the observation area only the wavefront can be seen through the window. When the imploding shock wave comes inside the observation area, not only the wavefront but also the region behind the imploding shock wave is seen and the average temperature becomes lower than the temperature at

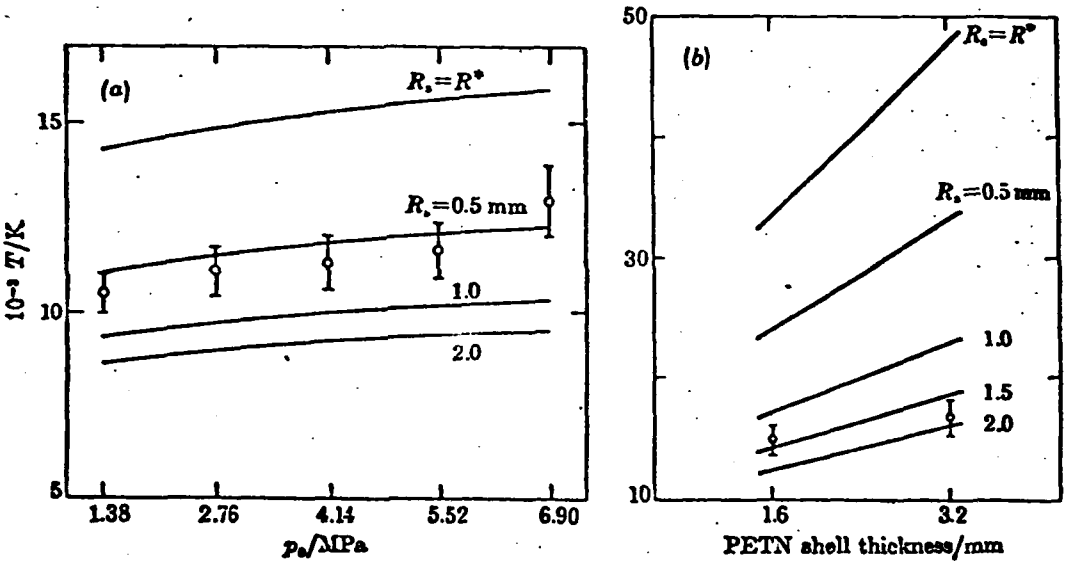

Figure 12. Comparison of experimental results with analysis for (*a*) gas runs and (*b*) explosive runs.

the wavefront. This arises from the rapidly falling temperature behind the implosion wave. As a result, the average temperature has a maximum when the radius of the imploding shock wave is slightly smaller than the radius of the observation area. The radius of the imploding shock at which this occurs is called R^*, as shown in figure 12. In other words, there is a certain maximum observable temperature for a certain size of observation area no matter how small the imploding shock wave becomes. This maximum temperature and the temperatures expected to be observed when the imploding waves are at different radii from the centre are also shown in figure 12. In principle, if it was possible to place the observation area exactly at the focus of the implosion then higher temperatures would be measured with decreasing

J. Fluid Mech. (1983), *vol.* 000, *pp.* 000–000
Printed in Great Britain

An update on non-stationary oblique shock-wave reflections: actual isopycnics and numerical experiments

By R. L. DESCHAMBAULT AND I. I. GLASS
Institute for Aerospace Studies, University of Toronto,
4925 Dufferin Street, Downsview, Ontario, Canada M3H 5T6

(Received 16 September 1982)

Nonstationary oblique shock-wave reflections over compressive wedges in air and argon were investigated using infinite-fringe interferometric techniques. These allowed direct, continuous and accurate observations of the isopycnics (lines of constant density) of the flow field. The initial pressures for these experiments were made as high as possible (30 to 250 torr) in order to increase the number of isopycnics and to enhance their details and distribution along the wedge surface over a shock-Mach-number range $2.0 < M_s \leqslant 8.7$. Included in the study were two cases of regular reflection (RR) and one of each of single-Mach reflection (SMR), complex-Mach reflection (CMR) and double-Mach reflection (DMR) for air, and one RR, SMR, CMR and DMR for argon. These particular cases, which we investigated previously in N_2 and Ar using a finite-fringe technique, have been used by computational fluid dynamicists to check their finite-difference results against our experimental data. It will be shown that the isopycnic structure previously reported by us differs in detail, in most cases, from that of the present study. The major difference arises from the fact that it was only possible previously to obtain discrete points on isopycnics and along the wedge surface. Consequently, the results obtained before were not as accurate. Comparisons were made of actual wall-density distributions with numerical simulations of the density contours of the various flows obtained by a number of authors. Each numerical method displays its advantages and disadvantages in describing the details of the flow fields. The present experimental results for air are new. They are of great interest from a practical viewpoint. The experiments in argon were redone to provide better data for a gas free from real-gas effects in the range of initial conditions considered, in order to simplify the computations in the numerical simulations. Although the recent numerical simulations are better than those reported previously, additional efforts are required to improve the predictions of the shape, location and values of the isopycnics and other flow isolines in the various regions and along the wall, and to render the predictions free of computer 'noise'. It is worth noting that real-gas effects did not play any role in determining the various transition lines of RR, SMR, CMR and DMR; a different claim was made in our previous work. Relaxation of nitrogen in air can be seen at the highest shock Mach numbers ($M_s = 7.19$ and 8.70), with relaxation lengths in good agreement with accepted predictions.

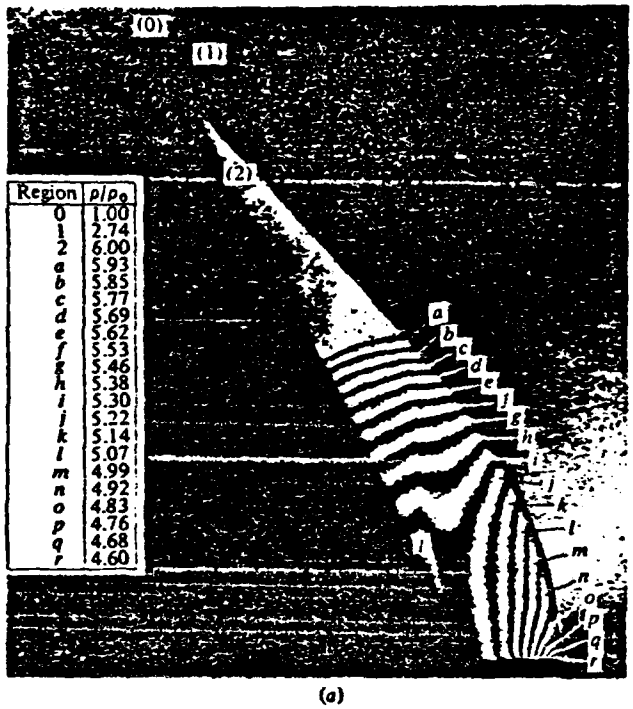
(0)
(1)
(2)
Region | ρ/ρ_0
0 | 1.00
1 | 2.74
2 | 6.00
a | 5.93
b | 5.85
c | 5.77
d | 5.69
e | 5.62
f | 5.53
g | 5.46
h | 5.38
i | 5.30
j | 5.22
k | 5.14
l | 5.07
m | 4.99
n | 4.92
o | 4.83
p | 4.76
q | 4.68
r | 4.60

(a)

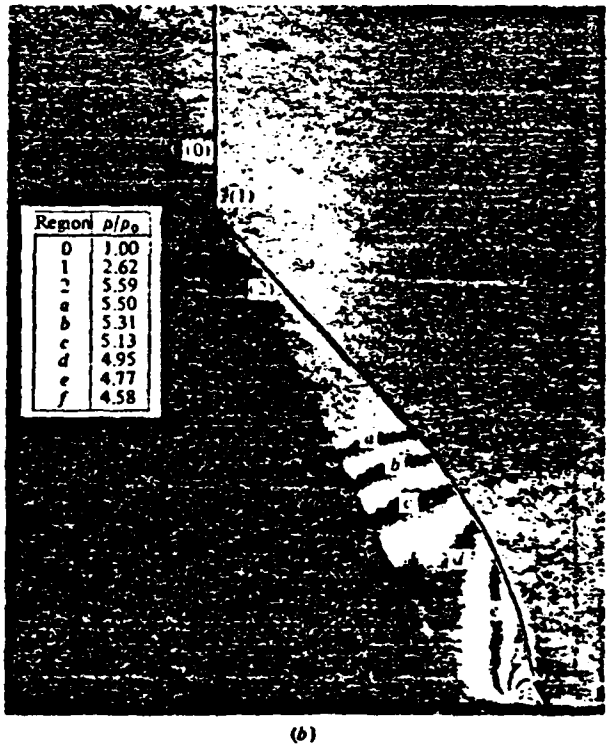
(0)
(1)
Region | ρ/ρ_0
0 | 1.00
1 | 2.62
2 | 5.59
a | 5.50
b | 5.31
c | 5.13
d | 4.95
e | 4.77
f | 4.58

(b)

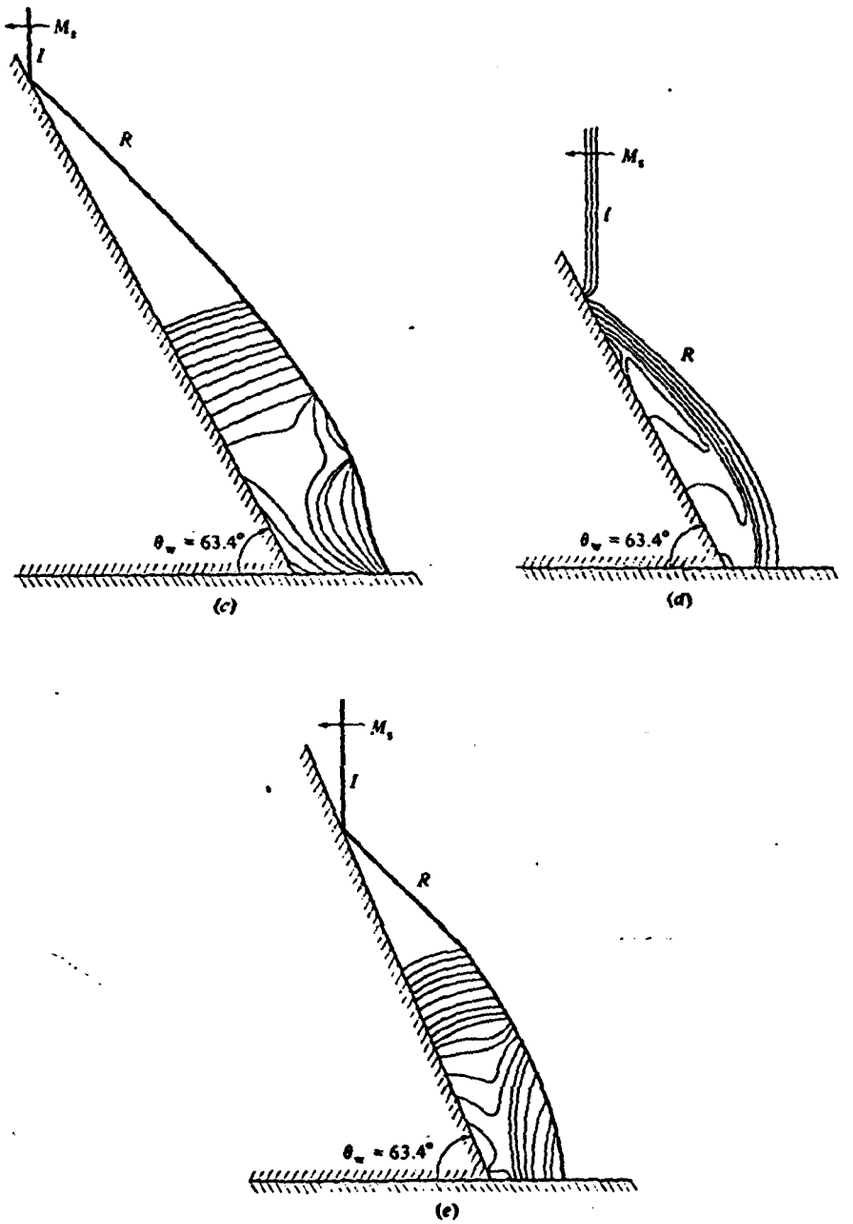

FIGURE 2. Isopycnics for regular reflection (case 1): (*a*) present experimental results, $M_s = 2.05$, $\theta_w = 63.4°$, $p_0 = 250$ torr, $\rho_0 = 3.87 \times 10^{-4}$ g/cm³, $T_0 = 298.4$ K, $\lambda = 6943$ Å; (*b*) Ando's (1981) experimental results in nitrogen, $M_s = 1.97$, $\theta_w = 63.4°$, $p_0 = 50$ torr, $T_0 = 298.2$ K, $\rho_0 = 7.58 \times 10^{-5}$ g/cm³, $\lambda = 3472$ Å; (*c*) isopycnics obtained from fringe-shift analysis of finite-fringe interferograms by Ben-Dor & Glass (1978), $M_s = 2.01$, $\theta_w = 63.4°$, $p_0 = 50$ torr, $T_0 = 298.6$ K; (*d*) numerical simulation of the contours of the density field by Schneyer (1975); (e) numerical simulation of the contours of the density field by Kutler & Shankar (1977).

INSTITUTE
FOR
AEROSPACE STUDIES
UNIVERSITY OF TORONTO

AN ASSESSMENT OF RECENT RESULTS ON PSEUDO-STATIONARY OBLIQUE-SHOCK-WAVE REFLECTIONS

by

M. Shirouzu and I. I. Glass

November, 1982

UTIAS Report No. 264
CN ISSN 0082-5255

Summary

The assumptions and criteria used in existing analyses in determining the regions and transition lines of pseudo-stationary oblique-shock-wave reflections have been re-examined in order to improve the agreement between experiments and computed data for regular (RR), single-Mach (SMR), complex-Mach (CMR) and double-Mach reflection (DMR).

It is shown that the relaxation lengths for vibration and dissociation determine whether frozen or equilibrium gas transition lines are applicable. For example, at an initial temperature of 300 K and a pressure of 15 torr (where much previous work was done) an equilibrium analysis would not be required for shock Mach numbers $M_s < 9$ [illegible] < 8 in air and $M_s < 3$ in CO_2.

Yet, the [illegible] data in N_2, CO_2 and very recent results for air, which are [illegible] the criterion (consistent with relaxation lengths) of the angle δ, between the incident and reflected shock wave, do not conclusively support the frozen or equilibrium gas calculations for N_2 and air. It does support CO_2 as an equilibrium gas contrary to a previous conclusion of agreement with $\gamma = 1.29$.

A new additional and necessary criterion for the transition from single to complex Mach reflection improves the agreement between analysis and experiment and is consistent with the requirements of the relaxation length and the angle δ. However, it now appears that a more accurate criterion is required for the boundary line between CMR and DMR.

A more detailed examination of the boundary-layer-displacement slope at the point of regular reflection appears to eliminate the so-called *von Neumann paradox*, and explains the persistence of regular reflection below the transition line for the occurrence of Mach reflection.

It is also shown that at the triple point the Mach stem can vary from being perpendicular to the wedge surface in actual experiments by as much as -3.0° to 7.5°. Consequently, calculations of the triple-point-trajectory angle χ on the basis that the stem is perpendicular is not always well founded.

It is verified that at lower shock Mach numbers M_s and large wedge angles θ_w, the experimental evidence shows that the transition lines for SMR ≠ CMR and CMR ≠ DMR converge at a point on the RR ≠ MR line, contrary to a previous simplified analysis.

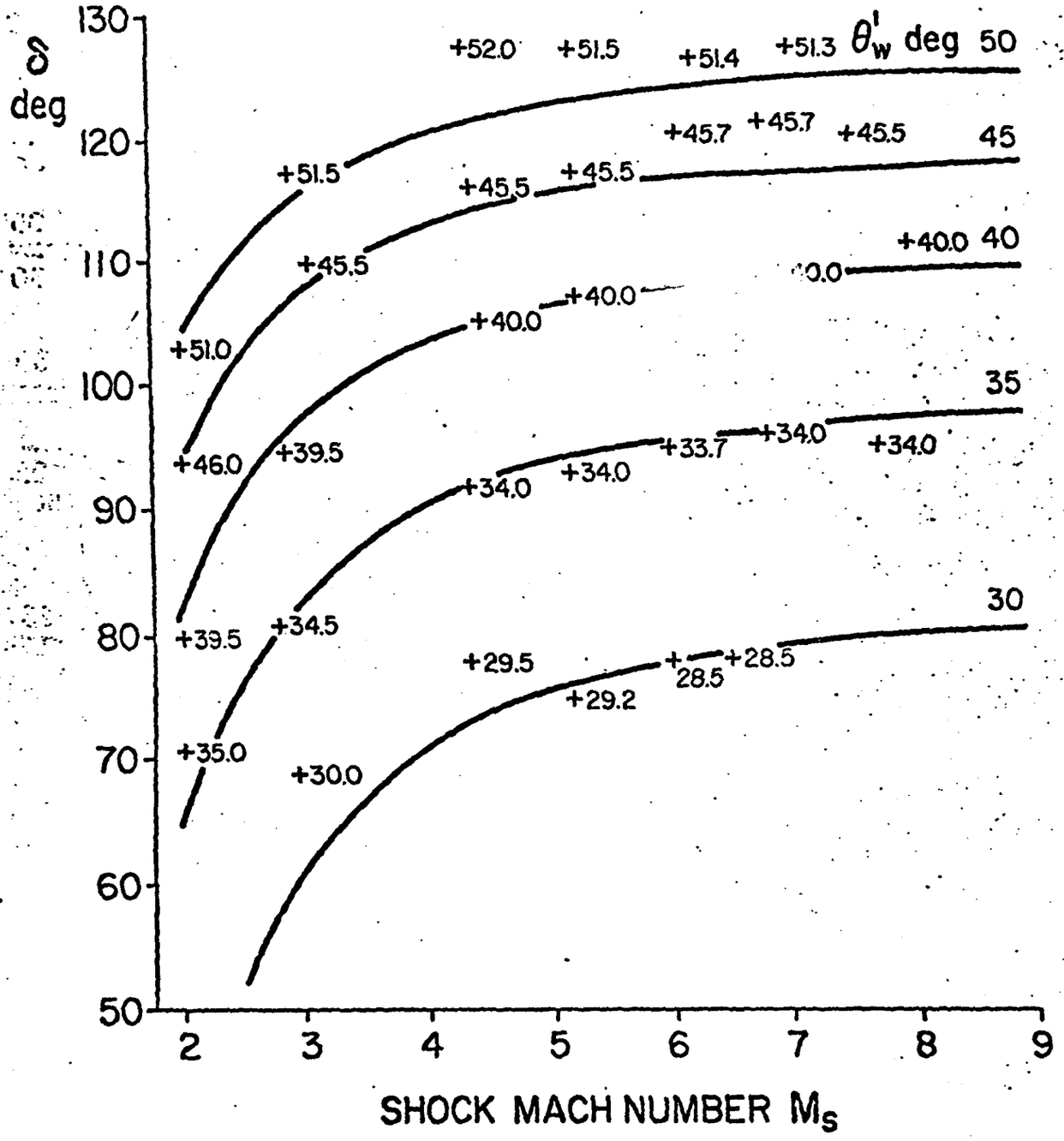

FIG. 15 VARIATION OF ANGLE δ VS SHOCK-MACH NUMBER AT FIXED θ'_w FOR Ar. ——— FROZEN Ar ($\gamma = 1.667$), + EXPERIMENTAL DATA FOR θ'_w (REF. 4).

INSTITUTE
FOR
AEROSPACE STUDIES
UNIVERSITY OF TORONTO

DOMAINS AND BOUNDARIES OF PSEUDO-STATIONARY OBLIQUE SHOCK-WAVE REFLECTIONS IN AIR

by

J.-H. Lee and I. I. Glass

June, 1982

UTIAS Report No. 262
CN ISSN 0082-5255

Summary

The reflection of oblique shock waves in air in pseudo-stationary flow was investigated analytically and numerically. The transition boundaries between the four types of shock-wave reflection (regular RR, single Mach SMR, complex Mach CMR and double Mach DMR) were established up to $M_s = 20$ for both perfect and imperfect air in thermodynamic equilibrium (rotation-vibration coupling, vibrational excitation, dissociation, electronic excitation and ionization). In addition, an analysis was made for perfect gases with differing γ, in order to clarify the effects of the specific-heat ratio γ, on the shock-wave configurations. It was verified that the reflected wave angle ω' was a very sensitive function of γ, and a decrease in γ lowered the value of ω' significantly and even shifted the value of ω' towards negative values under certain conditions of Mach reflection. This phenomenon occurred in a perfect gas with γ less than 1.4 and in imperfect air. However, it was absent in perfect air with $\gamma = 1.4$. [illegible] ion of the perfect and imperfect air results shows [illegible] transition lines and removes the conjecture of [illegible]-Mach reflection.

The present analytical results were compared with the available experimental data for air and nitrogen for shock Mach numbers up to 10. From the available experimental cases, it was clarified, by examining the relaxation lengths behind the shock waves, that the flow states behind the shock fronts, which determined the wave systems for the shock-wave reflection, were frozen or nearly frozen regarding vibrational excitation and dissociation. Consequently, in general, the present perfect-gas analysis agreed with experiment. However RR persisted, to some extent, below the perfect-gas termination line determined by the detachment criterion, and SMR and DMR did sometimes occur outside their analytically predicted domains. The development of more accurate transition criteria, improvements in the methods of predicting the first triple-point trajectory angle, accurate locations of the kink and triple points along with possible boundary-layer effects on the persistence of regular reflection are problems to be resolved in the future.

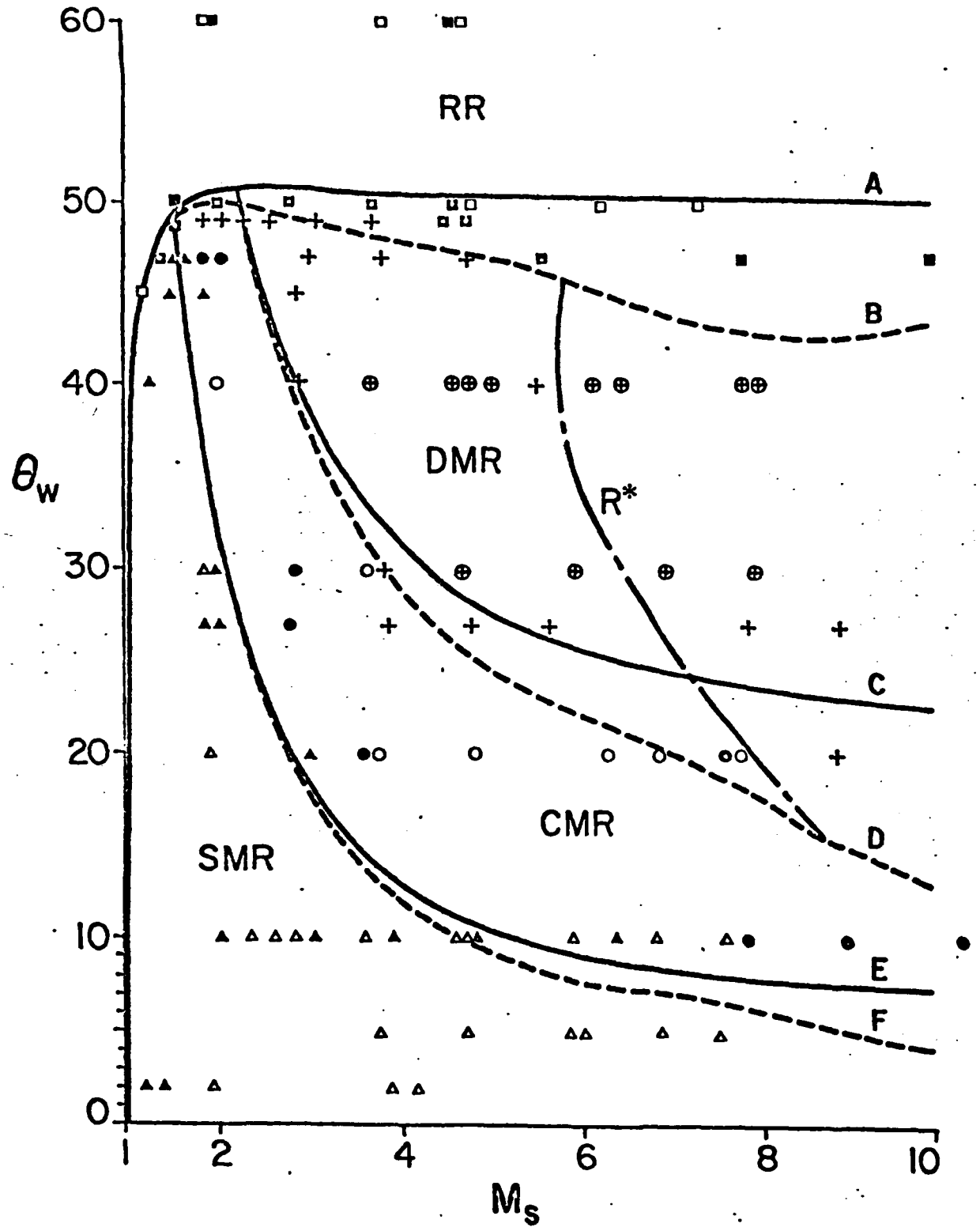

FIG. 23 COMPARISON OF PREDICTED DOMAINS OF VARIOUS TYPES OF REFLECTION AND THE EXPERIMENT IN THE (M_S-θ_W) PLANE. SOLID LINES ARE FOR PERFECT AIR WITH γ = 1.40. DASHED LINES ARE FOR IMPERFECT AIR AT P_0 = 15 TORR AND T_0 = 300 K. SOLID SYMBOLS ARE AIR DATA FROM DESCHAMBAULT [REF. 39]. OPEN SYMBOLS ARE N_2 DATA FROM BEN-DOR [REF. 40]. RR □■ , SMR △▲ , CMR 0 0, DMR ⊕ +.

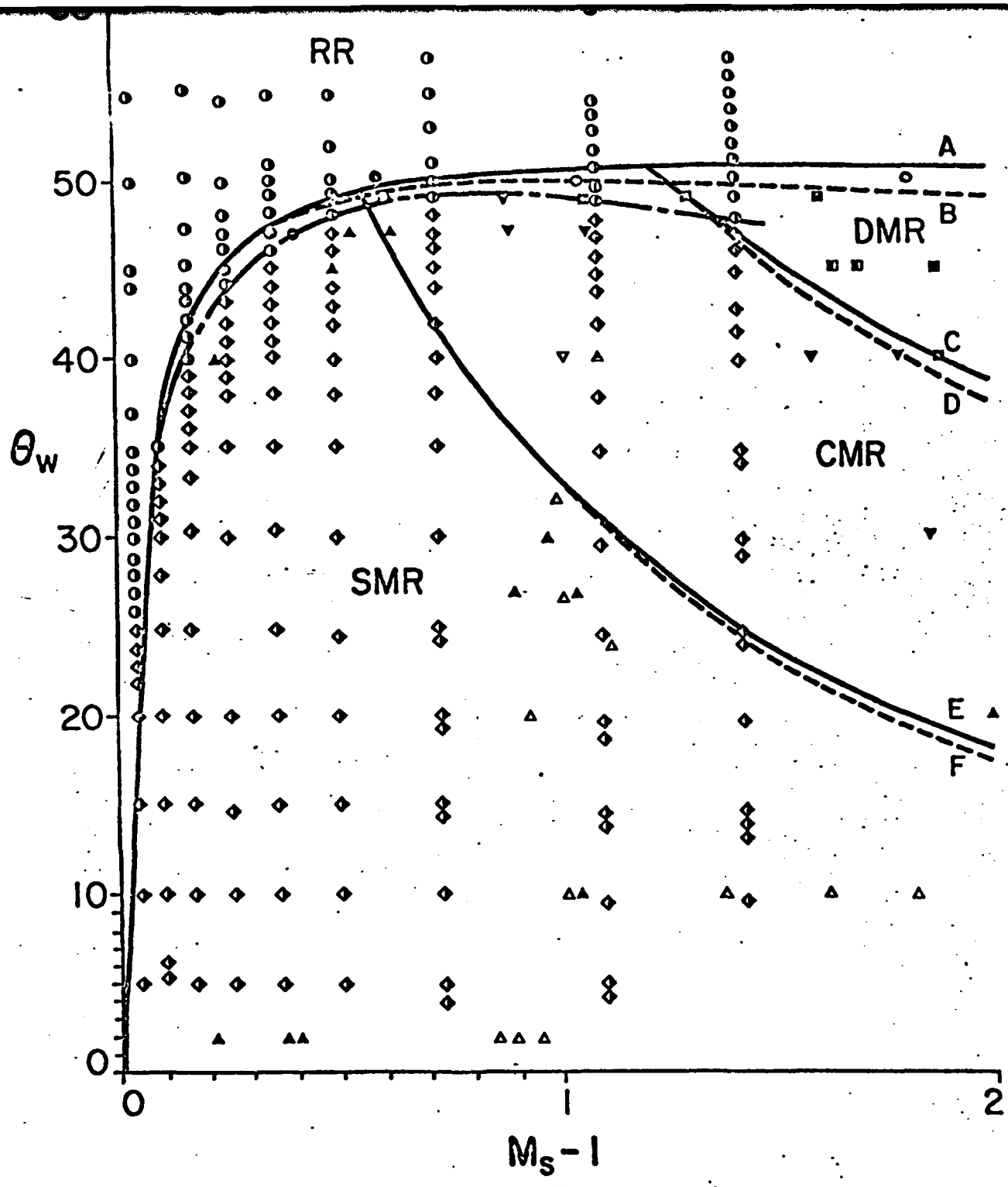

FIG. 24 COMPARISON OF PREDICTED DOMAINS OF VARIOUS TYPES OF REFLECTION AND THE EXPERIMENT IN THE (M_s-θ_w) PLANE IN THE RANGE $1.0 < M_s \leq 3.0$. SOLID LINES ——— ARE FOR PERFECT AIR WITH $\gamma = 1.40$. DASHED LINES ----- ARE FOR IMPERFECT AIR AT $P_o = 15$ TORR AND $T_o = 300$ K. DASH-DOT LINE —·—·— SHOWS PERSISTENCE OF REGULAR REFLECTION RR. EXPERIMENTAL DATA — AIR: SMITH 0 ◆ [REF. 9], BAZHENOVA ET AL ⊠ [REF. 18], DESCHAMBAULT ● ▲ ▼ ■ [REF. 39]; NITROGEN: BAZHENOVA ET AL ▲ [REF. 18], BEN-DOR 0 △ ▽ [REF. 40]; OXYGEN: LAW AND GLASS △ ▽ [REF. 19]. RR 0 0 0, SMR ▲ △ △ △ , CMR ▼ ▽ ▽ , DMR ■ ⊠ , MR ◆.

RANDOM-CHOICE SOLUTIONS FOR WEAK SPHERICAL SHOCK-WAVE TRANSITIONS OF N-WAVES IN AIR WITH VIBRATIONAL EXCITATION

by
H. Honma and I. I. Glass

Summary

In order to clarify the effects of vibrational excitation on shock-wave transitions of weak, spherical N-waves, which were generated by using sparks and exploding wires as sources, the compressible Navier-Stokes equations were solved numerically, including a one-mode vibrational-relaxation equation. A small pressurized air-sphere explosion was used to simulate the N-waves generated from the actual sources. By employing the random-choice method (RCM) with an operator-splitting technique, the effects of artificial viscosity appearing in finite-difference schemes were eliminated and accurate profiles of the shock transitions were obtained. However, a slight randomness in the variation of the shock thickness remains. It is shown that a computer simulation is possible by using a proper choice of initial parameters to obtain the variations of the N-wave overpressure and half-duration with distance from the source. The calculated rise times are also shown to simulate both spark and exploding-wire data. It was found that, in addition to the vibrational-relaxation time of oxygen, both the duration and the attenuation rate of a spherical N-wave are important factors controlling its rise time.

The effects of the duration and the attenuation rate of a spherical N-wave on its rise time, which are designated as *the N-wave effect* and *the nonstationary effect*, respectively, are discussed in more detail pertaining to Lighthill's analytical solutions and the RCM solutions for nonstationary plane waves and spherical N-waves. It is also shown that the duration and the attenuation rate of a spherical N-wave are affected by viscosity and vibrational nonequilibrium, so that they can deviate from the results of classical, linear acoustic theory for very weak spherical waves.

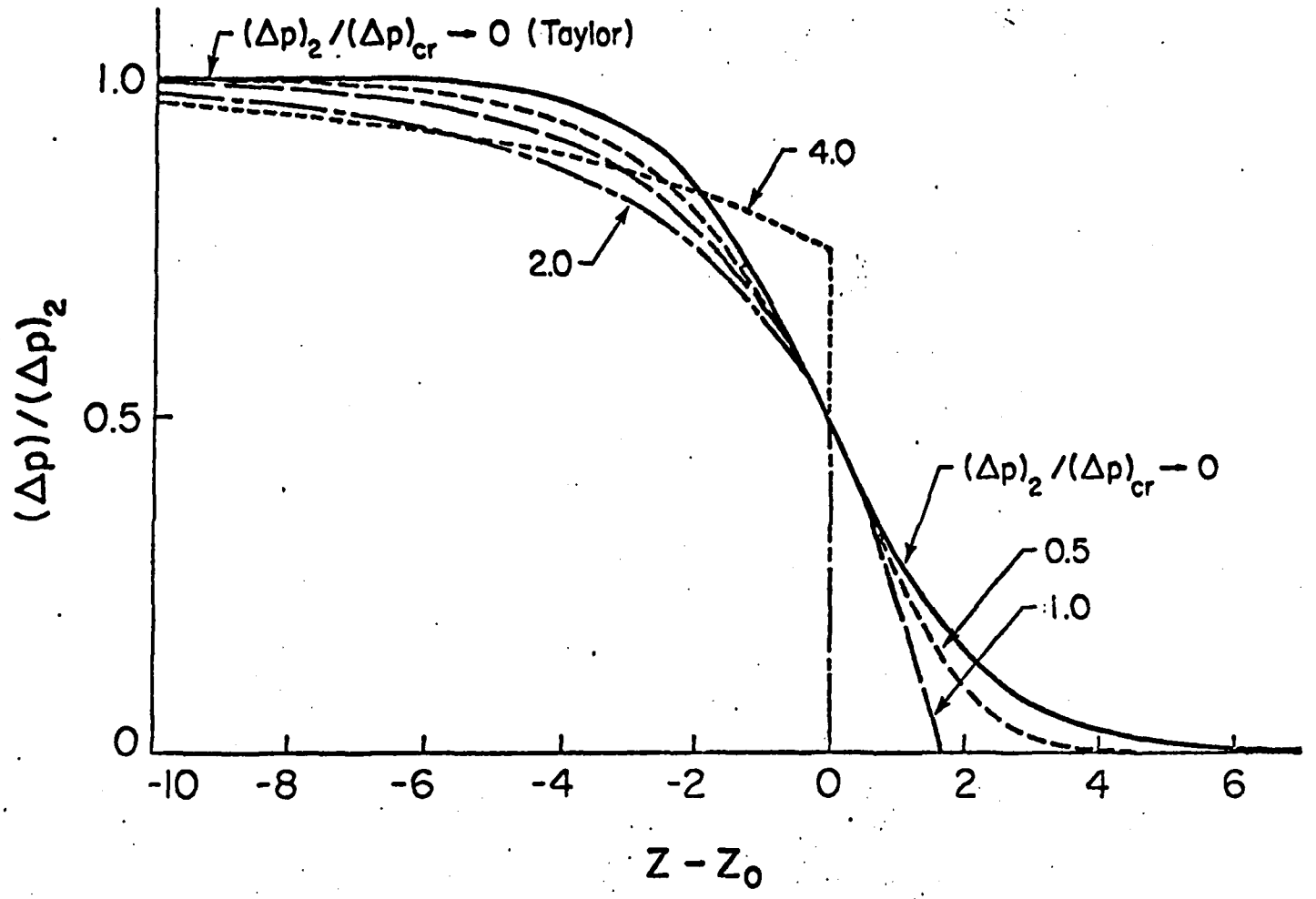

FIG. 3.16 PRESSURE PROFILES OF DISPERSED WAVES USING NORMALIZED OVERPRESSURE $(\Delta p)/(\Delta p)_2$ VS DISTANCE PARAMETER $Z-Z_0$ FOR OVERPRESSURE RATIOS $(\Delta p)/(\Delta p)_{cr,j}$ = 0, 0.5, 1.0, 2.0, 4.0.

INSTITUTE
FOR
AEROSPACE STUDIES
UNIVERSITY OF TORONTO

AN EXPERIMENTAL, ANALYTICAL AND NUMERICAL STUDY OF TEMPERATURES NEAR HEMISPHERICAL IMPLOSION FOCI

by

T. Saito

December, 1982

UTIAS Report No. 260
CN ISSN 0082-5255

SUMMARY

Spectroscopic temperature measurements in the visible radiation range were made near the focus of imploding shock waves in the UTIAS implosion chamber, which has a 20-cm diameter hemispherical cavity. The chamber was filled with a stoichiometric H_2-O_2 gas mixture at different initial pressures (13.6 ~ 68.1 atm). The mixture was ignited at the origin by an exploding wire generating an outgoing detonation wave which reflected at the chamber wall as an imploding shock wave (gas-runs). Additional experiments where an explosive shell of PETN was placed at the hemispherical wall were also conducted. The shell was detonated by the impact of the reflected gaseous detonation wave at its surface, thereby generating an intense implosion wave (explosive-runs). The continuous spectra and the measured emissivities, which were close to unity, confirmed the blackbody nature of the gas near the implosion focus. Temperatures were determined by fitting the measured radiation-intensity distributions to Planck's radiation distribution curve. They were 10,000 ~ 13,000 K for the gas runs and 15,000 ~ 17,000 K for explosive runs.

Semi-analytical solutions were developed by combining the solutions of the random-choice method (RCM) and the classical strong-shock theory of Guderley. The semi-analytical solutions provided a great deal of information on the entire implosion process within the restriction of a perfect-gas assumption which was found to be reasonable as a first step in this kind of analysis. The RCM alone detailed the ignition process of a PETN explosive shell at the hemispherical implosion-chamber wall and the subsequent complex wave interactions in that region.

A comparison between the analysis and the experiments showed that the observed temperatures for the explosive runs were limited to relatively

low values (15,000 ~ 17,000 K) owing to the screening effect of the preheated gas layers ahead of the radiating imploding shock waves, while they converged to very small radii.

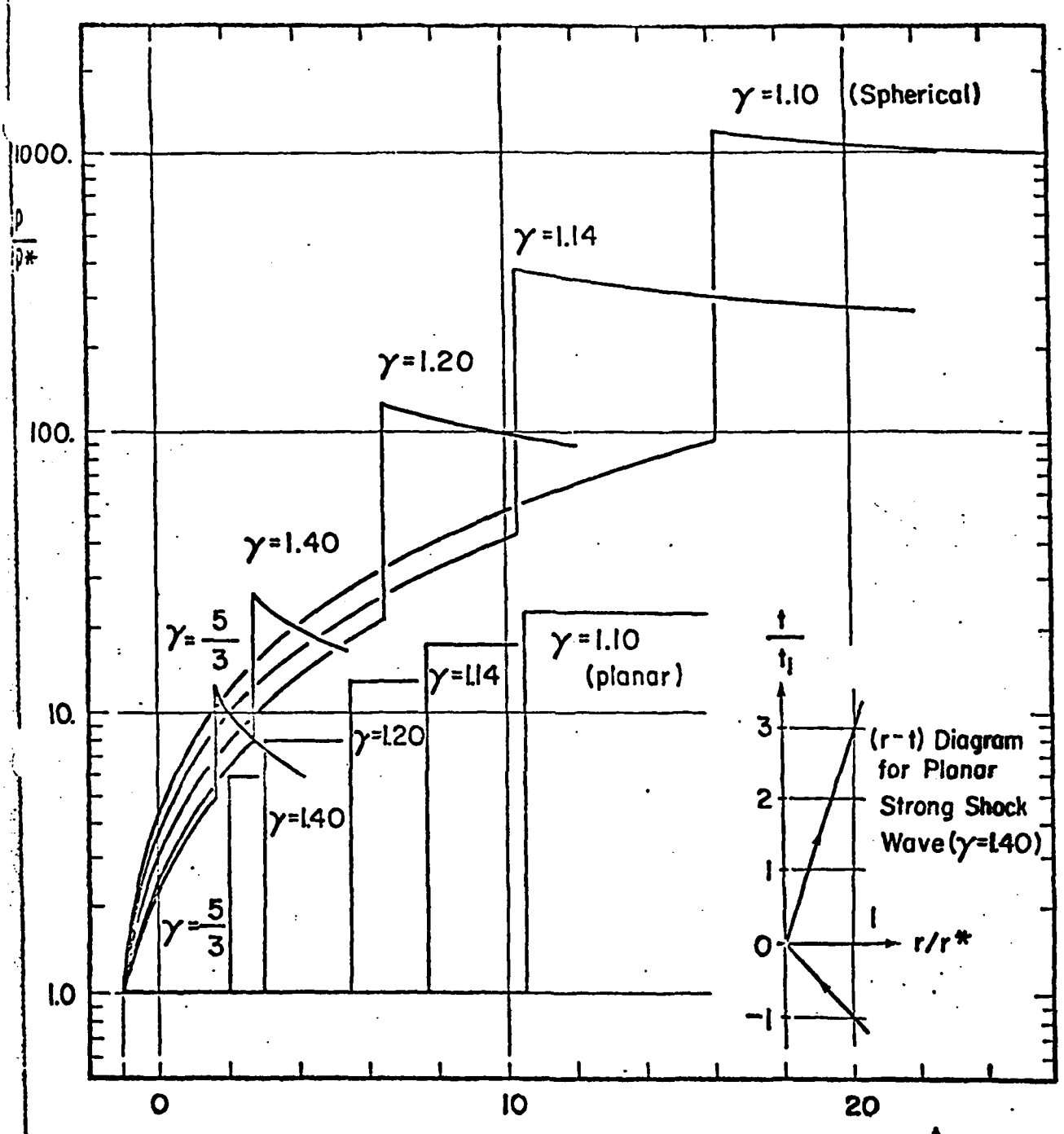

Fig. 34-a PRESSURE HISTORIES AT LOCATION r* FOR DIFFERENT γ'S (Guderley's Solution).

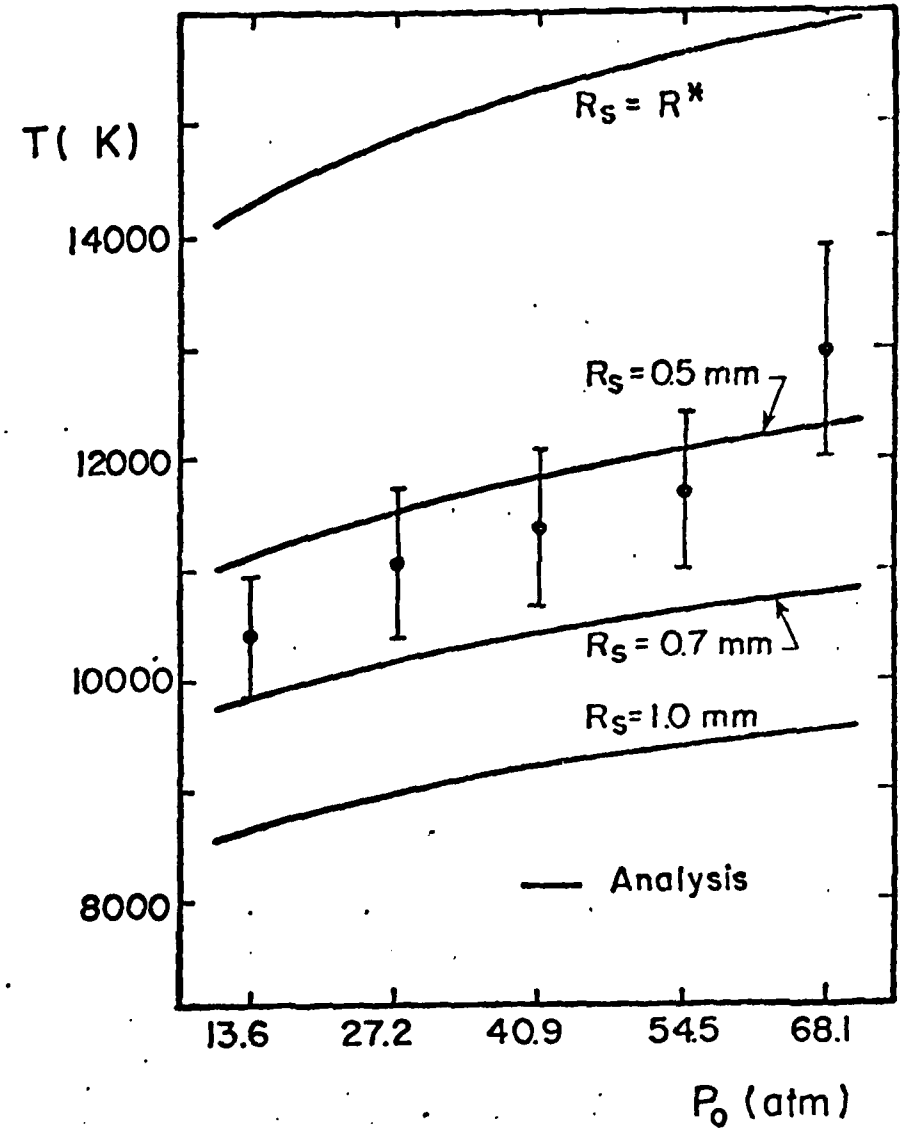

Fig. 76-a COMPARISON OF EXPERIMENTAL RESULTS WITH ANALYSIS FOR GAS RUNS.

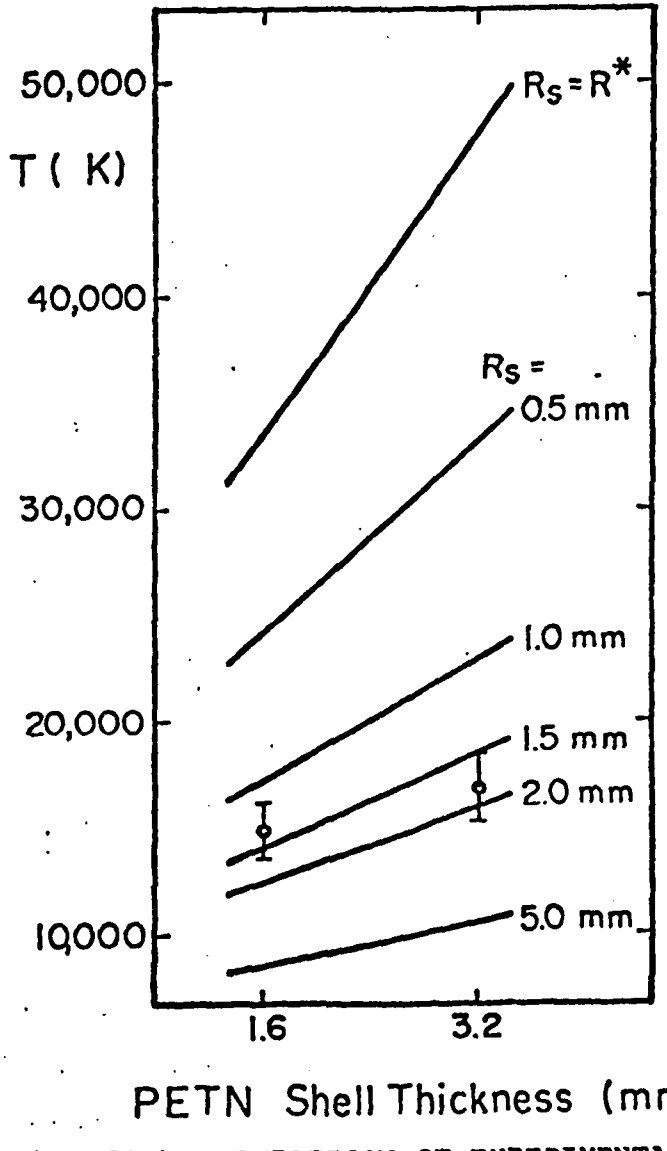

Fig. 76-b COMPARISON OF EXPERIMENTAL RESULTS WITH ANALYSIS FOR EXPLOSIVE RUNS.

NUMERICAL ANALYSIS OF DUSTY SUPERSONIC FLOW PAST BLUNT AXISYMMETRIC BODIES

by

H. SUGIYAMA

Submitted December, 1982

March, 1983

UTIAS Report No. 267
CN ISSN 0082-5255

Summary

An inverse method was developed for treating gas-particle supersonic flow past axisymmetric blunt bodies. This method is based on two transformations (von Mises and an additional one), which are convenient for determining the shock-layer flow fields and the body shapes.

In using the present method, the pure gas flow fields around spheres were first solved numerically for the freestream Mach numbers M_∞ = 10, 6, 4, 3, 2 and 1.5. These were found to be in very good agreement with the available results of Van Dyke and Gordon. Then the gas-solid-particle flow in the shock layer around blunt bodies (nearly spheres) were solved for the freestream Mach numbers M_∞ = 10 and 1.5, with freestream loading ratios α = 0, 0.2, 0.5 and 1.0 and particle diameters $\bar{d}_p$ = 1, 2, 5 and 10 μm, respectively. The effects of M_∞, $\bar{d}_p$ and α on the shock-layer thickness and the body surface pressures are discussed. The variations of the flow properties along the stagnation and adjacent streamlines are also shown in some detail.

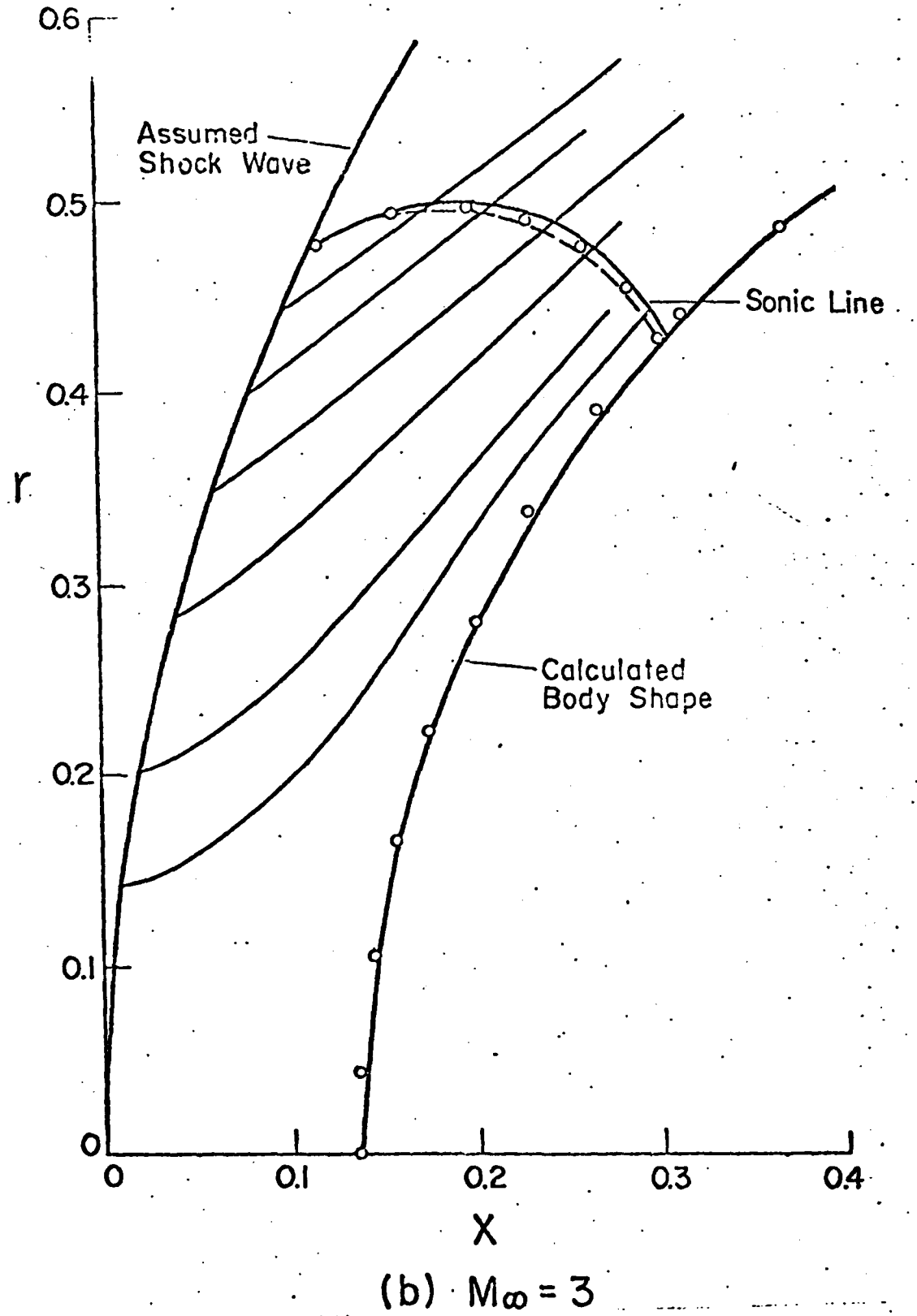

(b) $M_\infty = 3$

FIG. 2 SHOCK WAVE, SONIC LINE AND STREAMLINES FOR A SPHERE FOR PURE GAS, $\gamma = 1.4$. ⊖ VAN DYKE & GORDON [REF. 16].

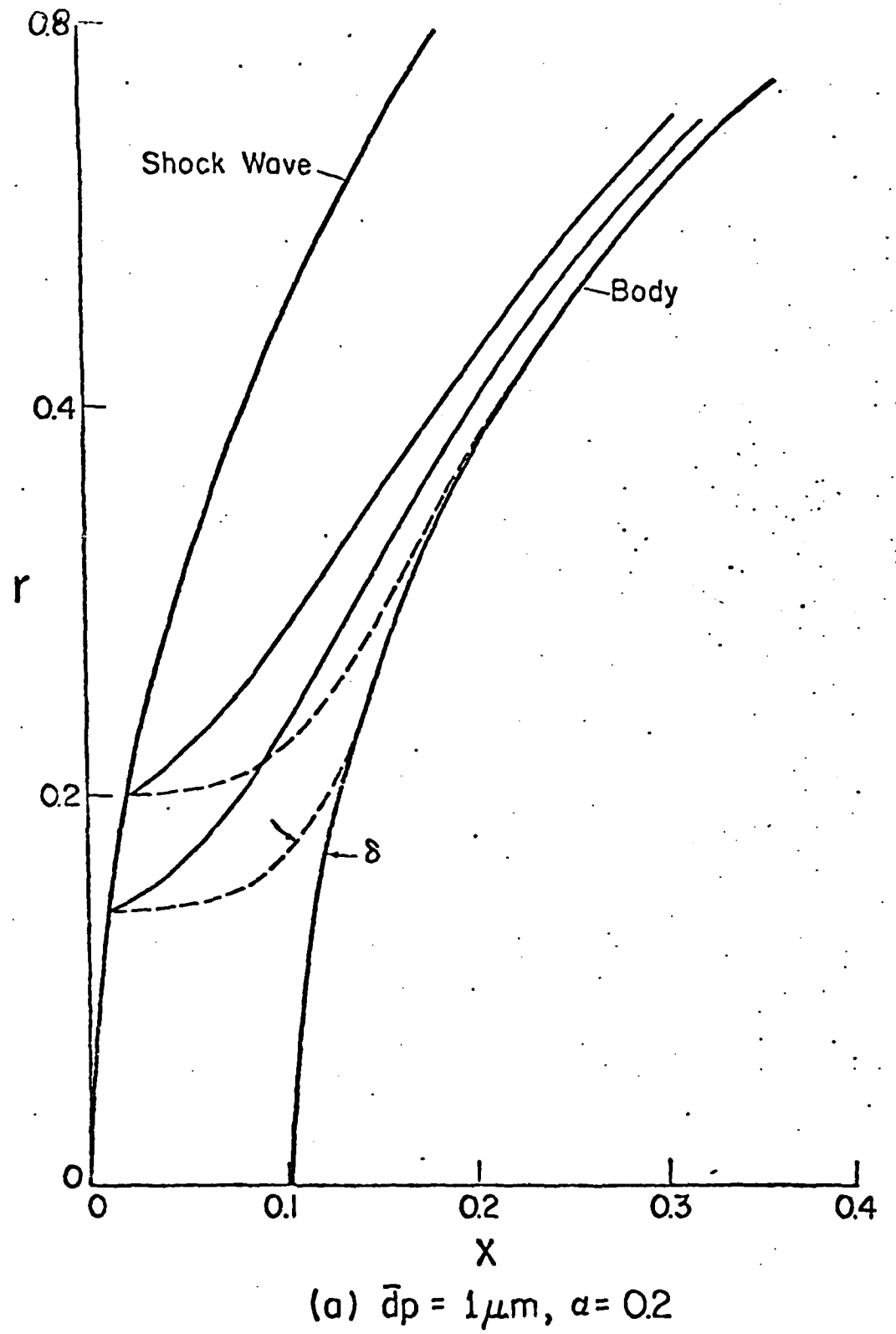

FIG. 10 GAS AND PARTICLE STREAMLINES AROUND BLUNT BODY FOR $M_\infty = 10$, $\bar{T}_\infty = 300$ K, $\bar{p}_\infty = 101.3$ KPa, $\bar{R}_S = 1$ CM: ——— GAS STREAMLINE, ------ PARTICLE STREAMLINE, IMPACT ANGLE δ.